Pergamon

Tetrahedron Letters 41 (2000) 2811–2815

TETRAHEDRON LETTERS

Solid-state and solution conformations of eleutherobin obtained from X-ray diffraction analysis and solution NOE data

Bruno Cinel,[a] Brian O. Patrick,[b] Michel Roberge [c] and Raymond J. Andersen [a,*]

[a]*Departments of Chemistry and Earth and Ocean Sciences, University of British Columbia, Vancouver BC V6T 1Z1, Canada*
[b]*Department of Chemistry, University of British Columbia, Vancouver BC V6T 1Z1, Canada*
[c]*Department of Biochemistry and Molecular Biology, University of British Columbia, Vancouver BC V6T 1Z3, Canada*

Received 22 January 2000; accepted 4 February 2000

Abstract

Single crystal X-ray diffraction analysis has revealed the solid-state conformation of the microtubule-stabilizing diterpenoid eleutherobin (**1**). NOE data obtained for **1** in $CDCl_3$ and DMSO-d_6 are consistent with solution conformations that are virtually identical to the solid state conformation.

Eleutherobin (**1**), initially isolated from a Western Australian octocoral in the genus *Eleutherobia* (possibly *albiflora*), represents one of a small number of antimitotic natural product families that are known to stabilize microtubules.[1] Other structural types possessing this important biological activity are represented by paclitaxel,[2] epothilones A and B,[3] discodermolide,[4] and the laulimalides.[5] The current excitement surrounding this group of compounds stems from the FDA approval of paclitaxel for the treatment of ovarian (1992) and metastatic breast cancers (1994). Paclitaxel's clinical utility has generated great interest in developing additional anticancer drug candidates that exploit its mechanism of action. One approach to designing the next generation of microtubule-stabilizing compounds has been to create three-dimensional pharmacophore models that embrace all the available SAR data for the known natural product structural types with these properties.[6,7] The validity of this approach has been demonstrated by the pharmacophore-guided design and subsequent synthesis of new hybrid structures with demonstrated cytotoxic and tubulin binding abilities.[6]

Creation of predictive pharmacophore models depends on detailed knowledge about the conformation of all the known structural types possessing microtubule stabilizing properties. To date, there have been no published solid-state or solution conformational analyses of eleutherobin (**1**), although the original report of the structure elucidation did provide a series of useful NOE constraints. Recently, we discovered that the Caribbean octocoral *Erythropodium caribaeorum* is a relatively high-yielding source

* Corresponding author. Tel: 604 822 4511; Fax: 604 822 6091; e-mail: randersn@unixg.ubc.ca (R. J. Andersen)

0040-4039/00/$ - see front matter
PII: S0040-4039(00)00269-0

of eleutherobin and several new structural analogs.[8] During the course of characterizing the antimitotic diterpenes from the *E. caribaeorum* extracts, several crystals of eleutherobin (**1**) were obtained by the fortuitous slow evaporation of a concentrated NMR sample dissolved in DMSO-d_6. The crystals proved to be suitable for X-ray diffraction analysis, which has provided the first solid state conformation for eleutherobin (**1**). ROESY and difference NOE data have also been collected for eleutherobin (**1**) in DMSO-d_6 and $CDCl_3$ in order to facilitate a comparison of the solid state conformation with the solution conformations in both a polar and a nonpolar solvent.

Eleutherobin (**1**) crystallized in space group $P2_12_12_1$ with a=12.8291(8), b=13.6209(6), and c=19.168(1) Å. A crystal with dimensions 0.30×0.20×0.15 mm, was mounted on a glass fiber. Data were collected at –100°C on a Rigaku/ADSC CCD area detector in two sets of scans (ϕ=0.0 to 190.0°, χ=0°; and ω=−18.0 to 23.0°, χ=−90°) using 0.50° oscillations with 58.0 s exposures. The crystal-to-detector distance was 40.55 mm with a detector swing angle of –5.52°. Of the 7035 unique reflections measured (Mo-Kα radiation, $2\theta_{max}$=55.8°, R_{int}=0.071, Friedels not merged), 4520 were considered observed ($I>3\sigma(I)$). The final refinement residuals were R=0.046 (on F, $I>3\sigma(I)$) and $wR2$=0.141 (on F^2, all data).[9] The data was processed using the d*TREK program and corrected for both Lorentz and polarization effects. The structure was solved by direct methods[10] and all non-hydrogen atoms were refined anisotropically, while all hydrogens involved in hydrogen-bonding were refined isotropically. All other hydrogens were included in calculated positions. The enantiomorph shown in Fig. 1 was chosen based on the known configuration of eleutherobin (**1**).[11] All calculations were performed using the teXsan[12] crystallographic software package of the Molecular Structure Corporation.

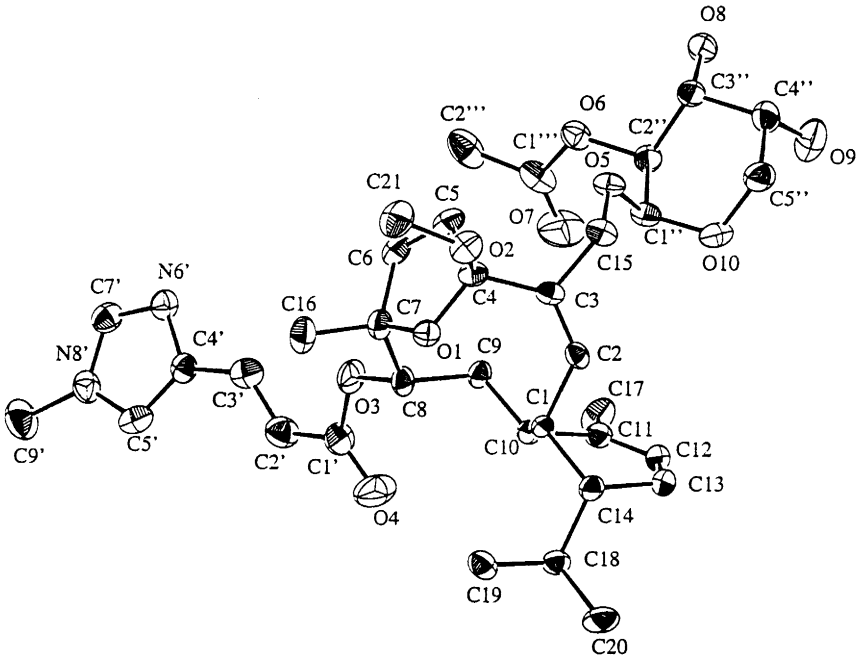

Fig. 1. ORTEP drawing of eleutherobin (**1**). Hydrogen atoms have been omitted for clarity

ROESY (500 MHz) and difference NOE (400 MHz) data were collected for eleutherobin (**1**) dissolved in DMSO-d_6 and $CDCl_3$. The NMR samples were degassed and purged of oxygen by freezing in a dry ice/acetone bath and placing the frozen sample under vacuum. The degassed samples were then flushed with argon and sealed. Table 1 lists the difference NOE results obtained in $CDCl_3$ and the ROESY

correlations observed in $CDCl_3$ and DMSO-d_6 along with the solid-state internuclear distances between the relevant pairs of protons. A number of key NOEs indicate that the solution conformation of the diterpenoid core of eleutherobin (**1**) in both $CDCl_3$ and DMSO-d_6 is identical to, or at least extremely similar to, the solid state conformation. These include difference NOEs observed in the resonances for H1, H10, and Me19 when the H8 resonance is irradiated and in H13α when H2 is irradiated. The C8–C9–C10–C1 torsional angle in the solid state is −66°, which places H8 2.438 Å from H1 and 2.304 Å from H10, consistent with the difference NOEs observed. A C9–C10–C1–C14 torsional angle of 177.7° in the solid state brings the Me19 protons into sufficient proximity to H8 to explain the weak difference NOE observed between their resonances, and the C2–C1–C14–C13 torsional angle of −61° in the solid state places H2 only 2.118 Å from H13α in agreement with the strong difference NOE observed between their resonances. Molecular models indicate that the combination of H8 to H10, H1, Me19 and H2 to H13α NOEs represent an extremely restrictive set of conformational constraints. Any significant deviation from the solid–state conformation results in H8 to H1, H10, Me19 and H2 to H13α interproton distances that would make the simultaneous appearance of the observed suite of NOEs between these protons highly unlikely. The diagnostic dipolar couplings between H8 and both H1 and H10, and between H2 and H13α, are all observed as ROESY correlations in both $CDCl_3$ and DMSO-d_6, providing additional evidence that the solution conformations in both solvents must be essentially identical to the solid-state conformation.

Table 1
Difference NOE[a] and ROESY[b] data for eleutherobin (**1**) in $CDCl_3$ and DMSO-d_6

H# (δ in $CDCl_3$)	H# (δ in $CDCl_3$)	Internuclear Distance from X-ray Data (Å)	Difference NOE (% enhancement) H in First Column was Irradiated	ROESY Correlations in $CDCl_3$	ROESY Correlations in DMSO-d_6
H2 (5.54)	H13α (2.29)[c]	2.12	7.49	y	y
H2	H14 (1.21)	2.61	3.51	y	y
H8 (4.80)	H1 (3.94)	2.44	4.28	y	y
H8	H10 (2.60)	2.30	6.16	y	y
H8	H16 (1.43)	2.52	0.91	y	y
H8	H19 (0.96)	2.64	0.52	y	n
H10 (2.60)	H1 (3.94)	2.33	4.79	y	y
H10	H8 (4.80)	2.30	2.61	y	y
H10	H19 (0.96)	2.51	0.77	n	n
H13α (2.29)[c]	H2 (5.54)	2.12	9.69	y	y
H14 (1.21)	H1 (3.94)	2.37	6.40	y	y
H19 (0.96)	H1	2.02	0.97	y	y
H19	H8 (4.80)	2.64	0.32	y	n
H19	H10 (2.60)	2.51	0.42	n	n
H20 (0.94)	H13β (1.97)[c]	2.03	0.96	y	y
OMe (3.20)	H16 (1.43)	2.28	1.01	y	y

[a] 400 MHz; [b] 500 MHz; [c] β and α are defined as being above and below the plane of the diterpenoid core of eleutherobin in the structural representation **1**; n - ROESY correlation not clear; y - ROESY correlation clearly observed.

It is interesting to compare the conformation of eleutherobin (**1**) revealed by the X-ray diffraction and solution NOE data in the current study to the conformation used by Ojima et al. in constructing their common pharmacophore for microtubule-stabilizing natural products.[6] In order to generate a

conformation for pharmacophore creation, Ojima et al. carried out molecular dynamic calculations on eleutherobin (**1**) without using any constraints. The exact coordinates for the resulting conformation that they used for **1** were not available, but Figure 4 in their paper indicates that the modeled conformation had a C8–C9–C10–C1 torsional angle of $>-90°$ and a C2–C1–C14–C13 torsional angle approaching 180°. A conformation with those torsional angles would not be expected to give any of the NOEs that are observed between H8 and H1 and Me19, or between H2 and H13α in $CDCl_3$ and DMSO-d_6. The Ojima conformation gives their binding region B (C11–C12–C13) a much different spatial relationship relative to the A (uroconic acid side chain) and C (D-arabinose residue) binding regions compared to the solid-state conformation (see Scheme 1). This suggests that the solid-state and solution conformations of eleutherobin (**1**) determined herein might have significantly different overlay fits with the reference structure nonataxel and the other microtubule-stabilizing structures that were used to construct the common pharmacophore. Therefore, it is anticipated that the availability of solid-state and solution conformation data for eleutherobin (**1**) will facilitate further refinements of microtubule-stabilizing pharmacophore models and, consequently, aid the eventual design of new compounds with this important biological activity.

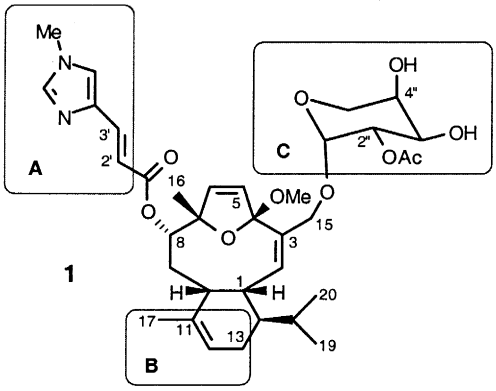

Scheme 1.

Acknowledgements

Financial support was provided by the Natural Sciences and Engineering Research Council of Canada (R.J.A.), the National Cancer Institute of Canada (R.J.A.), the Canadian Breast Cancer Research Initiative (M.R.), and the US Department of Defense Breast Cancer Program Idea Award No. DAMD17-99-1-9088 (M.R.).

References

1. (a) Lindel, T.; Jensen, P. R.; Fenical, W.; Long, B. H.; Casazza, A. M.; Carboni, J.; Fairchild, C. R. *J. Am. Chem. Soc*. **1997**, *119*, 8744−8745. (b) Long, B. H.; Carboni, J. M.; Wasserman, A. J.; Cornell, L. A.; Casazza, A. M.; Jensen, P. R.; Lindel, T.; Fenical, W.; Fairchild, C. R. *Cancer Res*. **1998**, *58*, 1111–1115.
2. Baloglu, E.; Kingston, D. G. I. *J. Nat. Prod*. **1999**, *62*, 1448–1472.
3. Bollag, D. M.; McQueney, P. A.; Zhu, J.; Hensens, O.; Koupal, L.; Liesch, J.; Geotz, M.; Lazarides, E.; Woods, C. M. *Cancer Res*. **1995**, *55*, 2325–2333.

4. ter Haar, E.; Kowalski, R. J.; Hamel, E.; Lin, C. M.; Longley, R. E.; Gunasekera, S. P.; Rosenkranz, H. S.; Day, B. W. *Biochemistry* **1996**, *35*, 243–250.
5. Mooberry, S. L.; Tien, G.; Hernadez, A. H.; Plubrukarn, A.; Davidson, B. S. *Cancer Res*. **1999**, *59*, 653–660.
6. Ojima, I.; Chakravarty, S.; Inoue, T.; Lin, S.; He, L.; Horwitz, S. W.; Kuduk, S. D.; Danishefsky, S. J. *Proc. Natl. Acad. Sci*., *USA* **1999**, *96*, 4256–4261.
7. Wang, W.; Xia, X.; Kim, Y.; Hwang, D.; Jansen, J. M.; Botta, M.; Liotta, D. C.; Snyder, J. P. *Org. Lett.* **1999**, *1*, 43–46.
8. Cinel, B.; Roberge, M.; Behrisch, H.; van Ofwegen, L.; Castro, C. B.; Andersen, R. J. *Org. Lett*. **2000**, *2*, 257–260.
9. Archival crystallographic data have been deposited with the Cambridge Crystallographic Data Centre, University Chemical Laboratory, Lensfield Road, Cambridge CB2 1EW, UK. Please give a complete literature citation when ordering.
10. Altomare, A.; Cascarano, M.; Giacovazzo, C.; Guagliardi, A. *J. Appl. Cryst*., **1993**, *26*, 343–350.
11. Chen, X.-T.; Bhattacharya, S. K.; Zhou, B.; Gutteridge, C. E.; Pettus, T. R. R.; Danishefsky, S. J. *J. Am. Chem. Soc*. **1999**, *121*, 6563–6579.
12. Crystal Structure Analysis Package, Molecular Structure Corporation (1985 and 1992).